ACS POLYMERS Au
AN OPEN ACCESS JOURNAL OF THE AMERICAN CHEMICAL SOCIETY

pubs.acs.org/polymerau
Article

Facile Method for the Preparation of Cyclodextrin-Rotaxanated Silicone Elastomers with Excellent Stretchability

Tao Xing,* Jiajun Ma, Wen-cong Xu, and Yangguang Xu

Cite This: ACS Polym. Au 2025, 5, 162−173
Read Online

ACCESS | Metrics & More | Article Recommendations | Supporting Information

ABSTRACT: Polysiloxane is an industrially important polymer, as it serves as the platform for the preparation of silicone materials with excellent thermal stability. Even though the fact that introducing rotaxanes into a polymer network provides a novel way to build new materials with peculiar mechanical properties is well-known, this tactic has rarely been applied to silicones, perhaps due to the lack of efficient synthetic methods. Here, in this work, we report the preparation and characterization of novel rotaxanated silicone elastomers by a simple two-step synthetic method. Starting from commercially available γ-cyclodextrin (CD) and vinyl-terminated polydimethylsiloxane, poly-[(dimethylsiloxane)-pseudorotaxa-(γ-cyclodextrin)]s were facilely prepared. These pseudopolyrotaxanes were then used to prepare silicone elastomers of different structures and compositions. Mechanical tests of these elastomers show that they have moderate tensile strength but an excellent extension ratio (∼800% for the sample with the highest extension ratio). γ-CD plays a unique and important role in shaping the network's topological structure and mechanical properties. This role was unveiled by applying various techniques such as solid-state NMR measurements and cyclic tensile tests to the elastomers obtained. Due to the simplicity of the current method, it may be used for large-scale preparation of stretchy silicone rubbers with optimum mechanical properties.

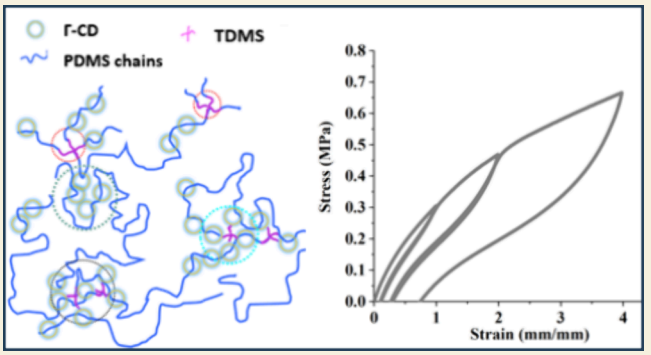

KEYWORDS: *polyrotaxane, polysiloxane, elastomer, stretchability, DQ-NMR*

INTRODUCTION

Main chain polyrotaxanes are a class of topologically interesting polymers with multiple ring molecules threaded on a backbone polymer. Among all the polyrotaxanes reported, cyclodextrin (CD)-based polyrotaxanes have attracted a lot of attention in recent years due to their facile preparation and wide applications.[1−4] CD has been reported to be able to complex with various types of polymers such as polyethylene glycol (PEG),[5,6] polybutadiene,[7] and polyurethane[8] to form pseudopolyrotaxanes. End-capping and cross-linking these pseudopolyrotaxanes readily give rise to topologically interlocked networks (also known as slide ring materials).[9,10] Compared with networks with fixed cross-links, cross-links formed by linking CDs are mobile because CDs are able to diffuse along the polymer backbone in slide ring materials. These unique mobile cross-links play the role of redistributing stress when the network is under large deformation. Since this redistribution homogenizes chain deformation, a direct result of this stress redistribution is a very large extension ratio for slide ring materials. Another result of the mobile cross-link, although not very intuitive, is that it creates networks with very low modulus.[11−13] Among various types of CD-based polyrotaxanes reported so far, PEG/α-CD type polyrotaxanes have been most popular and have been used to construct super stretchable hydrogels,[14] elastomers[9,10,15] and aerogels.[16]

Polydimethylsiloxanes (PDMS) are a class of industrially important polymers with excellent thermal and chemical stability.[17] These polymers have traditionally been cured to make silicone rubber, silicone foam, and silicone coating. However, polysiloxane-based polyrotaxane networks have rarely been prepared. Kato et al. reported the synthesis of the PDMS/γ-CD type slide ring gel.[18] In their work, polysiloxane was first complexed with γ-CD, followed by end-capping and cross-linking to make slide ring gels. However, no mechanical tests were performed on the slide ring gels obtained. Tran et at. prepared slide ring silicone elastomers by cross-linking hydrogen-terminated polysiloxane with vinyl-functionalized PEG/α-CD polyrotaxanes, and mechanical tests show that the obtained elastomers have relatively high extension ratio (250−400%) in comparison with

Received: December 5, 2024
Revised: February 27, 2025
Accepted: February 27, 2025
Published: March 7, 2025

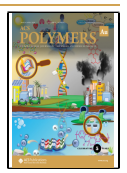

Figure 1. Structural illustration of slide ring elastomer with mobile cross-links and negligible filler−filler interactions and rotaxanated silicone rubbers with permanent cross-links and strong filler−filler interactions.

Sylgard 184 but low tensile strength (<1.2 MPa).[19] In the above two works, hydroxyl groups residing on cyclodextrane were masked to improve solubility and reduce the aggregation of CD mediated by hydrogen bonding. Actually, acetylation is usually regarded as a key step in making slide ring elastomers because CD clusters are usually bonded by extensive hydrogen bonding; bonded CDs are immobile and would terminate any stress distributions.[9,15,20,21] However, masking also reduces chain interactions and gives low-mechanical-strength materials with very limited use. Other problems with the rotaxanated silicones reported so far, in addition to their nonsatisfactory mechanical strength, include their multistep synthesis and noneconomical use of end-capping and acetylation reagents during preparation. Large-scale preparation of these materials is almost impossible, and the practical application of these materials is greatly restricted.

Here, in this work, a new method was developed to prepare rotaxanated silicone elastomers; elastomers with both large stretchability and optimal mechanical strength could be obtained by an economical two-step procedure. To prepare rotaxanated silicone elastomers, vinyl-terminated PDMSs were first complexed with γ-CD to prepare poly[(dimethylsiloxane)-pseudorotaxa-(γ-cyclodextrin)]s (PRs) of different structures and compositions. The obtained pseudopolyrotaxanes could be facilely cross-linked by curing with tetrakis (dimethyl siloxy) silane (TDMS) to give rotaxanated silicone elastomers (ERs). A cartoon illustration of these ERs' structure is shown in Figure 1, and a cartoon structural illustration of conventional slide ring elastomers is also shown in Figure 1 for comparison. ERs are structurally more or less like traditional filled rubbers with permanent cross-links and filler (γ-CD)-filler interactions, with the key difference being the filler threaded into the network strand and providing strong filler-network strand interactions. Slide ring elastomers, on the other hand, do not share too many common features with traditional filled rubbers because of the absence of either permanent cross-links or filler−filler interaction in these elastomers. Cross-links in slide ring materials are mobile, and the filler−filler interaction is eliminated by masking. As we would find out later, the presence of both filler−filler interaction and filler-network strand interaction is the key to the high extension ratio for some ERs in this work. ER with a maximum stress of about 1.8 MPa and a maximum extension ratio of about 800% could be prepared by optimizing the composition of the PR used. Structures and properties of these obtained ERs were characterized by various techniques such as Fourier transform infrared (FT-IR) spectrometry, solid-state NMR (SSNMR), and cyclic tensile tests. The obtained results show these networks are highly heterogeneous with several types of cross-links contributing to their final elasticity. γ-CD clusters in these networks play an important role in improving their mechanical strength and extension ratio. While the enhancement in strength is easily understood by realizing the chain interactions γ-CD brought in, the unique way in which γ-CD clusters reorganize under stress gives the material a very large extension ratio. Our results show that a large extension ratio for rotaxanated elastomers does not have to be achieved at the cost of mechanical strength, as so far reported in the literature.

EXPERIMENTAL SECTION

Materials

Vinyl-terminated polysiloxane with M_w of 25 kDa was purchased from Sigma-Aldrich. γ-CD, toluene, and TDMS were purchased from Alfa Aesar. All other chemicals were purchased from Maclin Chemical Corporation (Shanghai, China) and used as received.

Characterization

General. Thermal gravimetric (TG) measurements were performed on a PerkinElmer Q800 thermal gravimetric analyzer (TGA). The measurements were performed from 20 to 500 °C under nitrogen with a flow rate of 20 mL/min, and the heating rate was set to 5 °C/min.

Rheological tests (frequency sweeps and temperature sweeps) were performed on a stress-controlled HAAKE MARS rheometer; a parallel plate with a 25 mm diameter was used for these tests. Specimens of 25 mm in diameter and 0.5 mm in height were punched out from a 0.5 mm thick sheet. Frequency sweeps were performed from 0.01 to 100 Hz at 298 K, with the strain amplitude set to 0.2%. Temperature sweeps were performed from 20 to 200 °C with a heating rate of 3 °C/min, frequency was set to 1.0 Hz, and strain amplitude was set to 0.2% for these tests.

FT-IR spectroscopy measurements were conducted on a Nicolet Model 8700 Fourier transform infrared spectrometer. KBr disks with a diameter of 8 mm and a height of 1 mm were used for measurements, and the sample content was ∼5 wt %. A total of 64 scans from 500 to 4000 cm^{-1} were performed for each test.

Small-angle X-ray scattering (SAXS) measurements and wide-angle X-ray scattering (WAXS) measurements were performed on an Anton Paar GmbH (Austria) SAXSess system with an image plate detector. For each measurement, a test specimen with a thickness of about 0.5 mm was mounted in the sample chamber using Kapton tape. SAXS and WAXS patterns were recorded with scattering vector q from 0.08 to 2.26 nm^{-1} and 1.8 to 24.5 nm^{-1}. X-ray was generated by a copper anode operating at 40 kV and 50 mA, and the wavelength of the X-ray generated is 0.154 nm.

Uniaxial tensile tests and cyclic stress−strain tests were carried out on the Shimadzu EZ-SX tensile testing machine. Samples used for these tests were prepared according to procedures described in standard GB/T 528-92; procedures described in this standard were also adopted for the uniaxial tensile tests and cyclic stress−strain tests. For uniaxial extension, at least five specimens were stretched, and the test results (maximum stress and strain at break) were reported as average with standard deviation. Young's moduli were obtained by linear fitting the initial part (λ < 2%) of the stress−strain curves.

https://doi.org/10.1021/acspolymersau.4c00096
ACS Polym. Au 2025, 5, 162−173

Cyclic stress−strain tests were performed by sequentially stretching and releasing the sample to desired strains of 100, 200, and 400% for ER1−ER3. For the recovery tests, samples (ER1−ER3) were first subjected to an extension of 400%, strain was then released, and the stretched samples were left undisturbed at room temperature for different times (20 min, 3 and 10 h). At each predetermined time interval, the specimens were sampled for another round of extension of 400%, and the stress−strain curve was recorded.

Filling Ratio Determination. Due to the solubility difference between PDMS and γ-CD, the composition of PR could be determined by extraction using an organic solvent, which can selectively extract one component (in this case PDMS). Mole ratios of the two components were then used to calculate the filling ratio for each sample.[22] To determine the rotaxane content for each sample, a weighed amount (m_1) of the sample was loaded into a Soxhlet extractor, and then PDMS in the sample was extracted over a period of 16 h with toluene. After extraction, toluene was vaporized, and the residue was weighed (m_2). The filling ratio was then calculated using the formula below:

$$f = \left(\frac{m_1 - m_2}{m_2}\right) \times 0.092 \tag{1}$$

Sol Fraction. Sol usually refers to linear and branched polymers that are not connected to the infinite rubber network.[23] In our samples, sols refer to fractions (pseudopolyrotaxane, γ-CD, and polysiloxane) that could be removed by sequential extraction with toluene and ethanol. Samples were first swelled in toluene to extract PDMS, followed by swelling in ethanol to remove free γ-CD. In the case when the polyrotaxane is connected to the network by PDMS at one end, extraction with ethanol would remove γ-CD and give a bare dangling PDMS strand.

In a typical example, about 1.0 g (m_1) of sample was weighed into a 20 mL vial, and 15 mL of toluene was added. The vial was then sealed and held at 50 °C. After 10 h, toluene was discarded, and 15 mL of ethanol was added; the vial was held at 50 °C for another 10 h. The above process was repeated once again before drying the extracted sample in nitrogen flow, and the final mass of the sample was recorded (m_2). The sol fraction was then calculated using the formula below:

$$\omega_{sol} = \frac{m_1 - m_2}{m_1} \tag{2}$$

For the control PDMS elastomer without γ-CD, only extraction with toluene at room temperature was performed.

Solid State NMR Experiment. ^{1}H magic angle spinning (MAS) NMR measurements were performed on Bruker Avance III HD 600 MHz spectrometers by using 3.2 mm MAS probes. The samples were packed in 3.2 mm rotors in an argon-filled glovebox and were spun at 12 kHz during NMR measurements. Spectra were processed using the Bruker TopSpin software, and ^{1}H MAS NMR was performed using an excitation pulse (2.4 μs, 40 w) at resonance frequencies of 599.8 MHz. Samples were referenced to adamantane (1.8 ppm) in all cases.

Low field ^{1}H NMR experiments were performed on a Bruker Minispec mq20 spectrometer at a proton resonance frequency of 20 MHz with a typical π/2 pulse length of 3 μs and receiver dead time of about 13 μs. Because of the dead time of the receiver, initial decay signals related to fast relaxing components are usually not accessible by the free induction decay technique. However, this problem can be tackled by using a magic sandwich echo pulse (MSE, shown in Figure 2) which could refocus the initial FID signal.[24] A Hahn echo pulse sequence could eliminate magnetic field inhomogeneity and refocus the chemical shift anisotropy. A full FID decay was obtained by combining MSE FID at a short acquisition time (~80 μs) with a ^{1}H Hahn echo decay signal at a long echo time (80−10^6 μs).

The fully refocused FID decay obtained could be fitted to a combination of Weibullian functions. For polymer composite, the following equation with three components is usually used[25,26]:

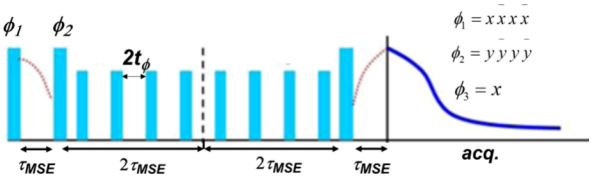

Figure 2. Magic-sandwich echo (MSE) pulse sequence for refocusing the loss of the rigid-phase signal due to the dead time.

$$I(t) = f_r \times \exp(-(t/T_{2r})^{\beta r}) + f_i \times \exp(-(t/T_{2i})^{\beta i}) + f_m \times \exp(-(t/T_{2m})^{\beta m}) \tag{3}$$

where f_r, f_i, and f_m are the fractions of the rigid, intermediate, and mobile components with corresponding apparent relaxation times T_{2r}, T_{2i}, and T_{2m}. For the β value, the decay signal of the rigid component could usually be fitted with a Gaussian function with $\beta_r = 2$, whereas an exponent β_m with a numerical value of 1 could describe the decay behavior of the mobile component. Intermediate values between 1 and 2 are often used to fit signals of intermediate components.

^{1}H DQ NMR is a robust and widely used technique for the investigation of polymer networks.[27−29] In DQ NMR experiments, usually, two sets of data are recorded. The first set is the decaying reference intensity I_{ref} which contains a signal from half of the quantum orders (4n) of the coupled network chains and a signal from uncoupled components. The second set is I_{DQ} which is dominated by spin-pair DQ coherences. The sum of the two components contains the full magnetization of the sample and is used at each excitation time τ_{DQ} to normalize the DQ build-up curve (eq 4).

$$I_{nDQ} = \frac{I_{DQ}}{I_{ref} + I_{DQ}} \tag{4}$$

Normalized I_{DQ} (I_{nDQ}, eq 4) is independent of the time scale of fast segmental fluctuations, leading to intensity decay at long times. Thus, the residual dipolar couplings that are representative of the network structure can be reliably accessed. The I_{nDQ} curve built in this way encodes the residual dipolar coupling constant D_{res} arising from the anisotropic orientation fluctuations of network chains. D_{res} and its standard deviation σ can be obtained by fitting the initial rise of the I_{nDQ} curve with eq 5.[30]

$$I_{nDQ}(\tau_{DQ}, D_{res}, \sigma) = \frac{1}{2}\left[1 - \frac{\exp\left(-\frac{\frac{2}{5}D_{res}^2\tau_{DQ}^2}{1+\frac{4}{5}\sigma^2\tau_{DQ}^2}\right)}{\sqrt{1+\frac{4}{5}\sigma^2\tau_{DQ}^2}}\right] \tag{5}$$

RESULTS AND DISCUSSION

Preparation and Characterization of PRs

PDMS is reported to be able to complex with γ -CD and β-CD to form pseudopolyrotaxanes.[22,31] For γ-CD, the complexation is fast even under heterogeneous conditions and is driven by the separation of products from the aqueous phase. A series of five pseudopolyrotaxanes were prepared by this method, and the recipes are shown in Table 1. Filling ratios of PR1-PR5 were determined by extraction with toluene, and the obtained results are also shown in Table 1; these results are in good agreement with filling ratios calculated based on feeding ratios. This is hardly surprising as filling ratios are low for these PRs, and the complexations are far from saturation. Note we keep the feeding ratios of γ-CD to relatively low values because powdered products start to form at high γ-CD loading (PR5). Powdered products cannot be effectively cured to give elastomers with optimal mechanical properties. In addition

https://doi.org/10.1021/acspolymersau.4c00096
ACS Polym. Au 2025, 5, 162−173

Table 1. Recipes for PRs Preparation and Composition of the PRs Prepared

sample	γ-CD content (wt %)		filling ratio (%)	
PR1	10.7[a]	9.8[b]	1.1[c]	1.2[d]
PR2	19.4	17.6	2.2	1.9
PR3	26.5	24.6	3.3	3.1
PR4	50.0	50.2	9.3	9.5
PR5	62.9	55.8	15.4	14.4

[a]Feeding ratio of γ-CD. [b]γ-CD content in PRs determined by TG. [c]Filling ratios calculated based on feeding ratio. [d]Determined by extraction.

to the method based on extraction, compositions of the obtained PRs could also be determined by TG.[18] TG curves of PRs, PDMS, and γ-CD are recorded (Figure S1), and the obtained results are used for the composition determination. Details regarding the calculation can be found in Supporting Information, and the obtained results are presented in Table 1. The γ-CD content determined by TG is in reasonable agreement with theoretical values, suggesting that complexation does not significantly alter the decomposition mechanism of γ-CD.

Structures of PRs were probed with FT-IR and ^{1}H MAS NMR, and the results are shown in Figures S2 and 3. While FT-IR spectra of PRs show two sets of peaks separately from γ-CD and PDMS (Figure S2) and provide little information about the PR formation. Evidence of PR formation could be found by a comparison of the ^{1}H MAS NMR spectra of PRs and BRs (prepared by mixing γ-CD with vinyl-terminated PDMS without solvent). In ^{1}H MAS spectra of BRs (Figure S3), as a result of the strong dipolar couplings between γ-CD protons, resonance peaks at ∼5 ppm are strongly broadened. For PRs, these hydroxyl proton peaks are significantly narrowed because threading γ-CDs into the mobile PDMS chain partially disrupts hydrogen bonding between γ-CDs and increases their ability to average dipolar coupling, and spectra with narrower peaks were therefore obtained for PRs.

Preparations of Rotaxanated Silicone Elastomers (ERs)

To prevent the dethreading of rotaxanes, end-capping of the backbone polymer with bulky groups is usually required.[6,18] However, due to the relatively low content of end groups for high molecular weight polymers, the yields of polyrotaxanes are low to moderate in most cases even though an excessive amount of end-capping agents is routinely used for end-capping.[32,33] This essential but very inefficient end-capping step greatly limits the scale of preparation and is one of several problems with traditional slide ring materials. In this work, end-capping and cross-linking were performed in one step by using TDMS as a curing agent (Scheme 1). After the reaction, γ-CDs threaded on PDMS strands were trapped by cross-linking points created during curing. Since the curing and end-capping were performed in bulk, dethreading is greatly suppressed, and all ingredients go to the final elastomers.

Structures and Properties of Rotaxanated Silicone Elastomers (ERs)

Mechanical properties of ER1−ER4 were measured by both quasi-static and dynamic mechanical tests. No mechanical test was performed for ER5 because it is brittle after curing and cannot withstand any tension or compression. Quasi-static mechanical performances of the obtained ER1−ER4 were evaluated by uniaxial extension, and the results are shown in Figure S4. Characteristic mechanical parameters extracted from curves in Figure S4 are collected in Table 2. With the increase of a γ-CD content in ERs, both modulus and maximum stress increase, as typically observed for filled rubbers. For maximum strain, no systematic change could be found, and there appears to be an optimal γ-CD content for the largest extension ratio. For traditional filled rubbers with fillers embedded in covalent networks, assuming fillers do not interfere with the formation of covalent cross-links, additional filler-network strand interactions impose extra restrictions on strands and lead to less deformable networks. For ERs in this work, end-capping and cross-linking were performed in one step, as we stated previously. The ratio of vinyl to dimethyl silane group (r) was kept to relatively higher values (larger than 3) to cure ERs so samples with optimal mechanical properties could be obtained. Since an excessive amount of TDMS was used, in addition to permanent cross-links by hydrosilylation, hydroxyl groups from γ-CD were also found to react with dimethyl silane to give Si−O−C-type cross-links. This type of reaction gives rise to H_2 as a byproduct, and the generated gas could easily be trapped in the cured silicone sheets. For thick sample curing at high temperatures, the

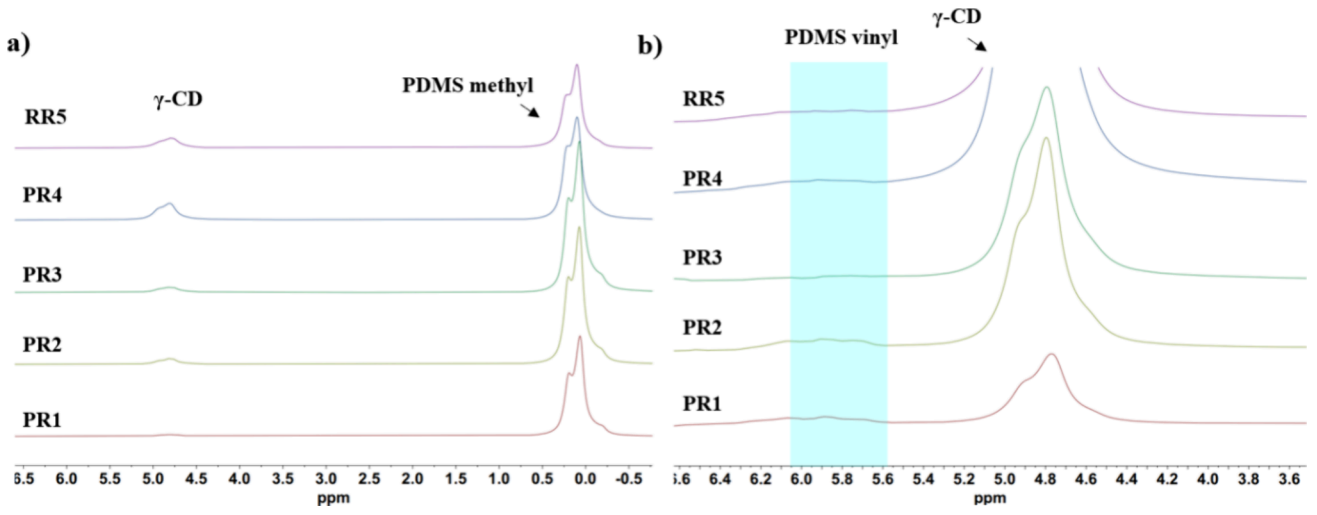

Figure 3. (a) ^{1}H MAS spectra of PRs acquired at a spinning speed of 12 kHz and (b) magnified image of the vinyl region in Figure 3a.

https://doi.org/10.1021/acspolymersau.4c00096
ACS Polym. Au 2025, 5, 162−173

Scheme 1. Synthesis of ERs by Hydrosilylation, Product Shown Is Connected to the Rest Part of the Network via Wavy Bonds

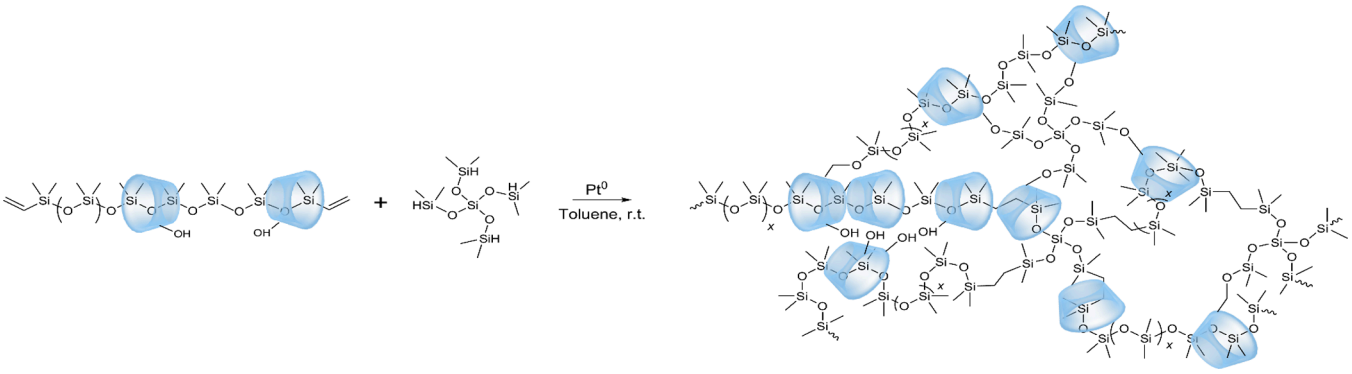

Table 2. Sol Fractions and Mechanical Parameters for ERs

	ER1	ER2	ER3	ER4	ER5	CR
sol (wt %)	3.5	5.3	5.9	7.2	9.8	4.3
σ_{max} (MPa)	1.06 ± 0.03	1.25 ± 0.13	1.79 ± 0.18	1.82 ± 0.23		0.47 ± 0.22
λ (mm/mm)	3.91 ± 0.28	7.91 ± 1.18	5.61 ± 0.99	0.88 ± 0.14		1.32 ± 0.31
E (MPa)	0.15 ± 0.02	0.24 ± 0.03	0.41 ± 0.05	0.62 ± 0.08		0.12 ± 0.03

curing reaction starts to give porous products. In order to eliminate these pores, only thin sheets (~500 μm) were prepared in this work. The cured networks are therefore featured by two types of cross-links formed by hydrosilylation between silane with vinyl groups (Si−$(CH_2)_2$−Si) and condensation between silane and hydroxyl groups (Si−O−C). From now on we will refer to them as type I and type II cross-links. For the unreacted hydroxyl groups, they are still linked by hydrogen bonds and form the third type of cross-links (physical cross-links). Strand deformation and the final extension ratio of ERs have complex dependence on the nature and relative amount of each type of above cross-links. Since quantifying the amount of each type of cross-link is difficult for ERs, the correlation of the strain behavior of ERs with their microstructure is impossible at this point.

With three types of cross-links presented, the topological structures of ERs are very complex, a very crude cartoon illustration of these networks is proposed in Figure 4. Ideal

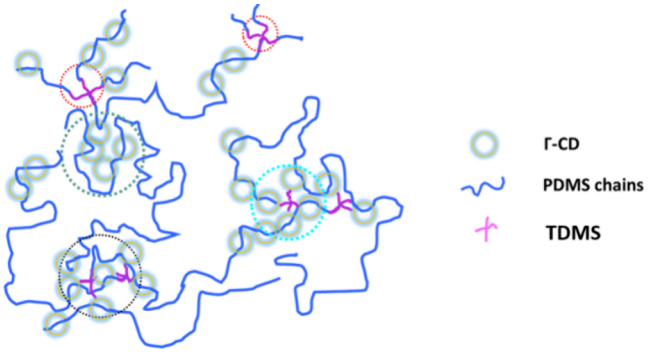

Figure 4. Cartoon illustration of the ER network.

cross-links created by hydrosilylation reactions alone have four arms emanating from TDMS (cross-links located in a red dashed circle). Cross-links created by condensations play the role in connecting γ-CD with themselves, and cross-links created by a combination of condensation and hydrosilylation play the role of linking PDMS strands with γ-CD (cross-links located within the light blue and black dashed circles, respectively). These cross-links are giant in nature as γ-CDs are predominantly linked by hydrogen bonds. For γ-CDs that are not covalently linked to PDMS, they are still connected by hydrogen bonds and are aggregates (shown in a green dashed circle). Loose chain ends may also exist in any of these γ-CD clusters. All of these cross-links are contributing to the elasticity of ERs, and they work cooperatively to determine the final mechanical behavior of ERs. In ERs, γ-CD and the PDMS matrix are in a phase-separated state due to their polarity difference; ER1-ER4 are thus translucent to milky white elastomers in appearance. For ER5, due to the high loading content of γ-CD, it is white powders and brittle solids before and after curing.

Several techniques, including SSNMR, have been employed to confirm the structures proposed in Figure 4. Structures of ERs were first characterized by solid-state ^{1}H NMR, and the results are shown in Figure S5. To reduce dipolar coupling and remove chemical shift anisotropy, the MAS technique was again applied.[34] ^{1}H MAS spectra acquired at a spinning speed of 12 kHz are shown in Figure S5. Two sets of peaks could be observed in these spectra: peaks located at ~0 ppm are related to methyl protons from dimethylsiloxane, and peaks located at ~4.6 ppm are related to protons from γ-CD. In contrast to spectra of PRs (Figure 3), peaks at ~6 ppm characteristic of vinyl protons disappear in Figure S5, suggesting the formation of type I cross-link by hydrosilylation. For γ-CD, very strong homodipolar coupling could only be partially removed by the MAS technique, and all its proton signals merge into one broad peak. A clear proton identification could not be made, and these spectra cannot be directly used for the structure identification to prove the existence of type II cross-links. However, the existence of type II cross-links could still be proved in indirect ways. For all ERs, gas release was observed during the curing process. Analysis of the released gas with gas chromatography shows it is hydrogen (Figure S6). For type I cross-links, in addition to ^{1}H MAS NMR results, their existence was also proved by a comparative experiment. A PR sample (DR4) was prepared by the same recipe used for preparing PR4 with trimethyl-terminated PDMS (22 kDa)

https://doi.org/10.1021/acspolymersau.4c00096
ACS Polym. Au 2025, 5, 162−173

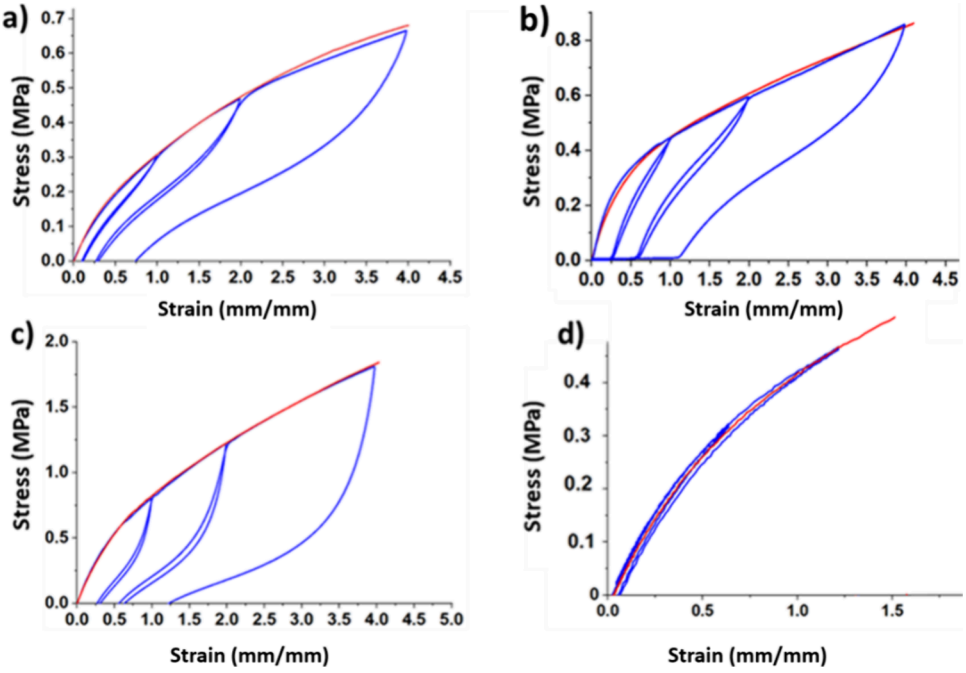

Figure 5. Sequential tensile strain cycles for ER1−ER3 (a−c) and control PDMS elastomer CR (d), first pull to 100%, second pull to 200%, and third pull to 400% for ERs and 50 and 100% sequential pull for CR. Also shown in each image is the stress−strain curve for a separate sample pulled to 400% (for ER1−ER3) and 155% (for CR).

instead of vinyl-terminated PDMS as an ingredient. This PR, as the curing reaction shows, could not be cured into nontacky elastomers (Figure S7). These results therefore indicate that type I cross-links must be playing an important role in shaping the mechanical properties of ERs in this work.

Mechanical performances of ERs were further evaluated by sequential extension-retraction cycles, and the experimental results are shown in Figure 5. ER4 is brittle with a maximum extension ratio of only 92% (Figure S4); cyclic extension is therefore not performed for this sample. The cyclic stress−strain curve of CR prepared by curing the same base vinyl PDMS used for preparing PR1−PR4 is also shown in Figure 5 as a comparison. Since CR is weak and cannot be stretched to large ratios, maximum strains of 50 and 100% were performed. ER1−ER3 are much stronger and tougher in comparison with CR. While they are of moderate mechanical strength, ER1−ER3 are very stretchy even in comparison with some slide ring elastomers.[15,35] For the slide ring material, the large extension ratio is usually ascribed to their unique topologically cross-linked structure. Under external stress, strained polymer strands move through cross-links (γ-CD) to reduce their deformation, and this strain redistribution prevents any individual chain from being overstretched and gives networks with a very large extension ratio.[12] However, this mechanism cannot be applied to ER1−ER3 to explain their large extension ratios because γ-CDs in ER1−ER3 are in the aggregated state. To elucidate the microstructures of these samples and aid the explanation for the large extension ratio, WAXS measurements were conducted to investigate the ERs. WAXS curves of ERs are similar in shape (Figure S8), suggesting these samples are similar in microstructures. To better analyze these scattering curves, the scattering results of CR and γ-CD are also shown in Figure S8. CR is amorphous and only has one broad scattering peak located at about 8.4 nm^{-1}. γ-CDs are crystalline and have multiple scattering peaks spanning from 3.5 to 21.8 nm^{-1}. Scattering curves of ERs, in addition to the broad peak centered at 8.4 nm^{-1} related to the PDMS matrix, are also characterized by sharp peaks with scattering vectors ranging from 5.3 to 18.9 nm^{-1}. These peaks correspond to d-spacing values from 0.33 to 1.18 nm and probably are due to lattice scattering or scattering from γ-CD clusters. Scattering curves of ERs are in stark contrast to scattering curves of polyrotaxanes with γ-CDs uniformly distributed along the polymer backbone, which usually are characterized by featureless broad peaks with small scattering vectors (larger d-spacing values).[9,10] In those polyrotaxanes, interactions between γ-CDs are reduced or eliminated by structural modifications (e.g., acetylation),[9,10,36] in ERs, hydrogen bonding persists after threading, and binding between γ-CDs is further enhanced by condensation. In addition to WAXS, SAXS was also applied to investigate ERs, as the test results show (Figure S9). The obtained curves are featureless with no scattering peak, suggesting in these samples no long-range periodicity of tens of nanometers size exists. This is probably because γ-CDs in ERs are in phase-separated aggregated states; these clusters are mediated by strong hydrogen bonding and randomly dispersed in the PDMS matrix. As a result of the strong interactions between γ-CDs, any chain length redistribution is prohibited in these irregularly shaped clusters; large extension ratios for ERs therefore must have a different structural origin. Another feature of curves in Figure 5a−c is the Mullins effect. Stress in each sample is reduced on subsequent extension up to the maximum previous strain. When we use an independent sample as a control, we note that for strains above the previous maximum, the stress rejoins the curve that would be observed for a continuous first extension. The Mullins effect has been observed in a lot of unfilled and filled rubbers, including PDMS.[37−39] Different mechanisms have been proposed by different researchers to explain their findings. For ER1-ER3, the Mullins effect observed is apparently related to γ-CDs threaded on the polymer backbone since the control CR network without γ-CD shows a negligible Mullins effect (Figure 5d). We envision that

https://doi.org/10.1021/acspolymersau.4c00096
ACS Polym. Au 2025, 5, 162−173

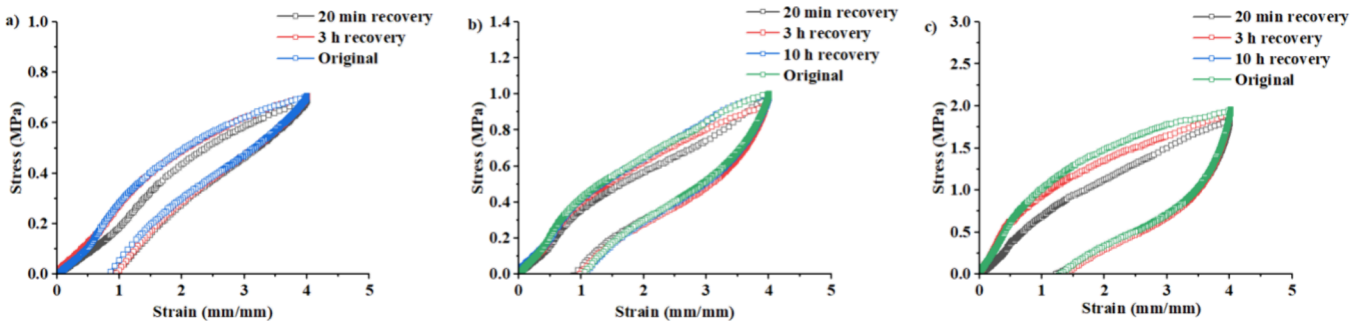

Figure 6. Stress−strain curves for ER1 (a), ER2 (b), and ER3 (c) recovered at room temperature for different times. For comparison, the stress−strain curve of an original sample was also shown.

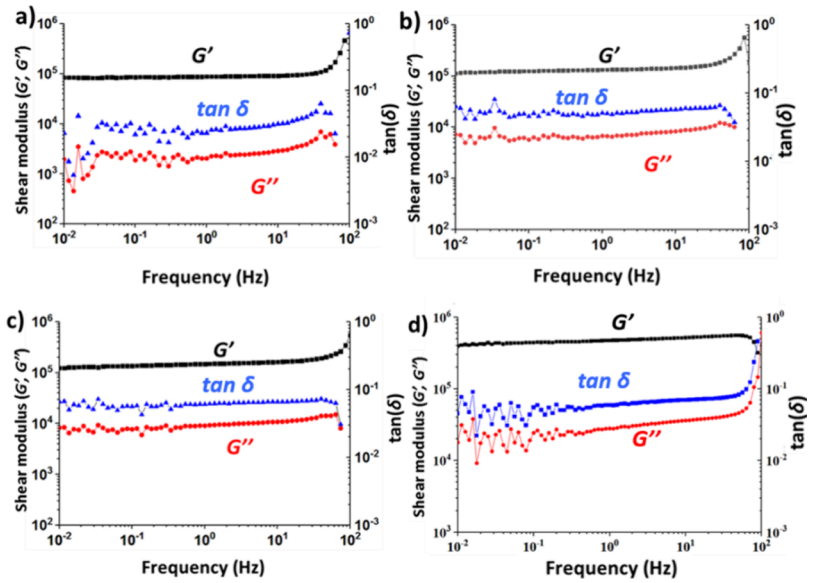

Figure 7. Storage modulus (G'), loss modulus (G''), and tan δ data for ER1−ER4 (a−d).

upon extension the hydrogen bonds between γ-CDs break, leading to the simultaneous release of stress and strain. New aggregates formed under external stress will not immediately go back to the previous equilibrium state once the strain is released; this leads to the permanent set and adherence to the release curve up to the previous maximum strain. The reorganization of γ-CD clusters, therefore, could be identified as the reason for the large extension ratio observed for ER1-ER3. It is interesting to note that since γ-CD threads on PDMS chains in ER1-ER3, γ-CD clusters in these samples must be interacting much more strongly with PDMS chains than found in traditional silicone rubber−filler systems. This strong interaction indicates the stress, which is initially supported by PDMS strands, could be effectively passed down to the surrounding clusters. These clusters then dissipate the energy received by breaking hydrogen bonds. This new way of homogenizing stress and strain gives these elastomers very unique mechanical properties (large extension). While in traditional slide ring materials, large extensions rely on complex synthesis and are accomplished at the cost of mechanical strength,[19] in this work elastomers with both a large extension ratio and optimum mechanical strength could be attained by a very simple method.

Further comparisons among curves in Figure 5a−c show that the permanent set after cyclic extension-retractions slightly increases with the augment of the γ-CD content in each sample. Note for CR without γ-CDs, a negligible permanent set can be seen after cyclic extension, suggesting chain deformations in covalently cross-linked networks are fully recoverable. For ERs in Figure 5, as we have stated above, stretching these samples causes reorganization of the γ-CD clusters and scission of hydrogen bonds. For samples with larger amounts of γ-CD clusters, it is natural to assume extension is accompanied by a larger amount of hydrogen bond scission and, in turn, a larger permanent set.

Since most elastomers in a practical lifetime would experience repeated extension and the working mechanism for a high extension ratio for ERs is the break of hydrogen bonds, a question naturally arises is that will extended ERs recover their stress−strain behavior after strain release? To answer this important question, ERs (ER1−ER3) were first subjected to an extension of 400%, and then the strain was released. The released samples were rested at room temperature for different times and then subjected to extension again. Stress−strain curves for the original sample and the recovered sample are shown in Figure 6. As we can see from the results, all samples recover their mechanical properties over time, stress−strain curves for ER2 and ER3 after 10 h resting are almost indiscernible from their original stress−strain curves, suggesting full recovery was accomplished within 10 h resting. For ER1, the recovery seems to be faster and completes within 3 h. Since rupture of covalent bonds is permanent and would

https://doi.org/10.1021/acspolymersau.4c00096
ACS Polym. Au 2025, 5, 162−173

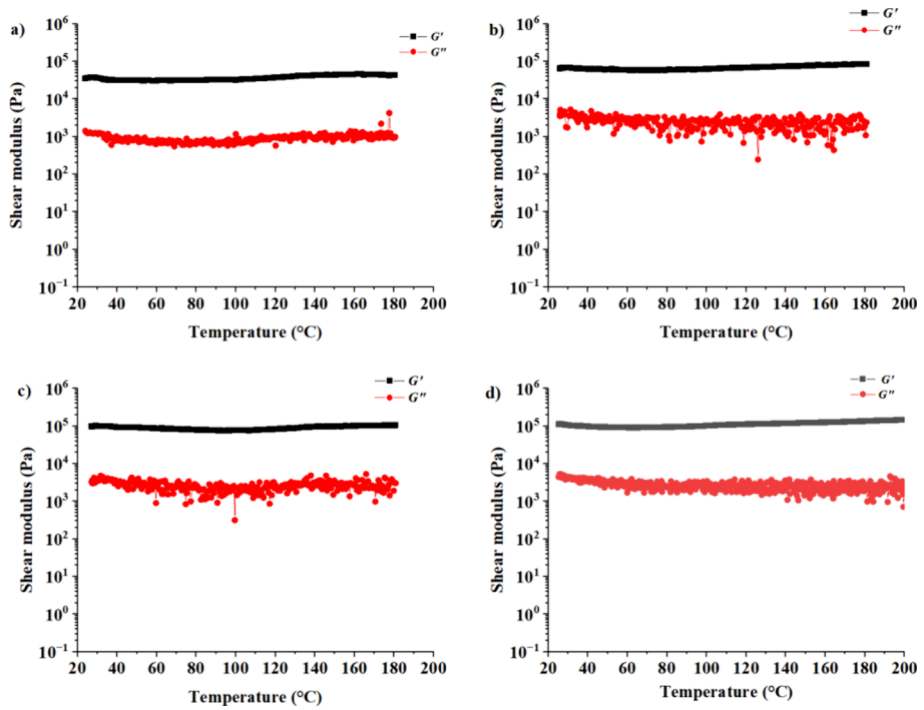

Figure 8. Temperature Ramps for ER1−ER4 (a−d).

lead to irreversible mechanical strength loss, the recovery results shown in Figure 6, therefore, suggest that no permanent cross-links break during strain extension of 400%. The hysteresis loop observed in Figure 5 is not a result of covalent bond rupture, as has been suggested in a recent report by Hagita et al.[40]

Dynamic mechanical properties of ER1-ER4 were probed with frequency sweeps. These measurements were performed from 10^{-2} to 100 Hz at room temperature, and the results are shown in Figure 7. Storage modulus (G') is larger than loss modulus (G'') for all samples, which is typical for elastic solids. The noise in G'' at low frequency is due to the usual difficulties in precision for determining a phase angle close to zero. The fact that the phase angle is close to zero ($G' \gg G''$) indicates that these samples are well cross-linked and contain only a small amount of imperfections such as sols.[41] In order to confirm this, the sol fractions of ERs were determined by repeated extraction. Since PDMS and γ-CD have very different solubilities. We first swelled the sample in ethanol at 50 °C to extract any free γ-CDs that might exist. The swelled sample was then immersed in toluene to remove free PDMSs and possible branched silicone molecules. Note any free PRs dethread during this process, and the generated PDMS and γ-CD would be extracted. Sol fractions obtained by this method are listed in Table 2. For ERs, the sol fraction in each sample tends to increase with γ-CD content; this probably indicates that for samples with higher γ-CD loading, the likelihood of TDMS to react with γ-CD to form type II cross-links is increased while the formation of type I cross-links is reduced. This in turn creates free PR chains not connected to the elastic network which could be removed by solvent. All samples have low sol content (<10 wt %), suggesting the cured networks contain relatively small amount of free γ-CDs and free polysiloxanes. These results also indicate dethreading is negligible when the curing reaction is performed in bulk. Since all samples were swelled in ethanol to remove γ-CD, small sol fractions also suggest that although Si−O−C-type links have been reported to be unstable in protic solvent and at high temperatures,[42,43] they are quite stable under the swelling conditions and cannot be broken by protic solvent such as ethanol.

The type II cross-links are reported to be dynamic and have been used in several cases to build malleable materials.[42,44] A question that arises is whether ERs are dynamic in nature. This question is of vital importance, as it dictates the way in which these materials could be used and processed. To answer this question, temperature sweeps for ER1−ER4 were performed, and the results are shown in Figure 8. All samples turn out to be quite stable to heating, with no noticeable modulus change upon heating to 200 °C. Since modulus scales proportionally with cross-link density ν ($G \sim \nu kT$) for rubber materials,[23] these results therefore suggest the type II cross-links that are contributing to elasticity are not undergoing thermal-initiated exchange reaction within the test temperature range. Actually, as the extraction test results show, ERs swelled in ethanol at 50 °C for 10 h show low sol fraction (Table 2), suggesting the type II cross-links are stable even in protic solvent conditions with moderate heating. Note that in addition to type II cross-links, hydrogen bonds between γ-CDs are also contributing to the elasticity of ERs. The fact that the moduli are not dependent on temperature in Figure 8, therefore, indicates that hydrogen bonding interactions between γ-CDs are strong, and in the test condition, these bonds show the property typically seen for covalent bonds. Actually, since the PDMS chain is very flexible with a glass transition temperature of about −120 °C, threaded γ-CDs in ERs could adjust their position to effectively bond with each other, threading γ-CDs into the PDMS chain does not significantly disrupt the hydrogen bonds formation between γ-CDs, and the bond strength is still strong in these elastomers.

To better understand the structure/property for these samples, two sets of solid-state NMR techniques were

https://doi.org/10.1021/acspolymersau.4c00096
ACS Polym. Au 2025, 5, 162−173

employed to investigate these samples. The first set is the MSE-refocused FID, and the second set is MQ NMR. These two techniques study component mobility at different time scales and have been used in combined ways to give a whole picture of polymer dynamics at different length scales.[26,45−48] Information extracted from NMR experiments can be linked to specific polymer structures and further used to construct a structure−property relationship for polymer materials. MSE-refocused FID signals for ERs are shown in Figure 9. Due to

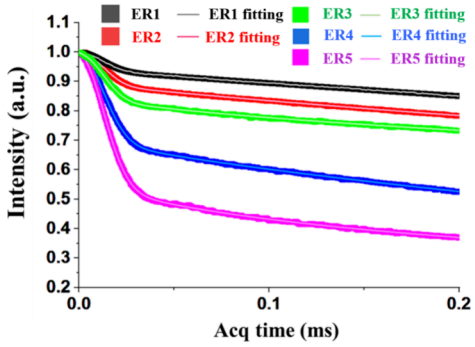

Figure 9. MSE-refocused FID signals as a function of the acquisition time for ERs.

the much stronger dipolar couplings of the rigid γ-CD aggregates compared with flexible PDMS chains, FID signals of ERs all show a two-step decay with different slopes. The fast decay appears at a short time scale and is due to the relaxation of the rigid component (γ-CD aggregates). This fast decay is followed by a slow decay happening over a relatively long time scale.

MSE-refocused FIDs usually can be fitted with a combination of stretched or compressed exponential (Weibullian) functions $e^{-(t/\tau)^{\beta}}$. For a rigid polymer, β is usually set to 2 (Gaussian relaxation), while for a mobile elastomer, β is usually set to 1 (exponential relaxation). Depending on the exact structure of the sample, other Weibullian functions with β values between 1 and 2 could also be used in combination to achieve better fittings. For ERs in this work, as we can see from Figure 9, MSE-refocused FID signals could be well fitted by a combination of three Weibullian functions with $\beta = 1$, $\beta = 1.5$, and $\beta = 2$. Quantitative fitting to eq 3 gives the transverse relaxation time (T_2) and the relative fraction of each component (f); these results are summarized in Table 3. Rigid fractions monotonically decrease, while mobile fractions increase with the decrease of γ-CD content in ERs, and this is in agreement with the sample design as shown in Table 1. As for the intermediate fractions, no clear dependence of f_I on the recipe can be seen. ER1-ER4 have f_I of a few percent, while ER5 has very large f_I of about 25%.

Table 3. Component Fractions and Transverse ^{1}H NMR Relaxation Times Obtained by Fitting of MSE-Refocused FID Signals Shown in Figure 9

sample	f_r (%)	T_{2r} (ms)	f_i (%)	T_{2i} (ms)	f_m (%)	T_{2m} (ms)
E1	6.14	0.018	4.38	0.059	89.48	1.80
E2	11.44	0.018	2.06	0.051	86.50	1.92
E3	16.18	0.017	2.35	0.061	81.47	2.02
E4	27.42	0.018	4.70	0.033	67.88	1.78
E5	41.99	0.018	24.46	0.14	33.55	2.02
CR			1.14	0.62	98.86	2.01

Another useful parameter that could also be extracted by fittings is the transverse relaxation time T_2. In polymer materials, constraints such as cross-links and entanglements slow or inhibit the averaging of ^{1}H−^{1}H dipolar couplings and yield transverse ^{1}H relaxation times (T_2), which correlate with the extent of cross-linking and macroscopic mechanical properties.[49−52] Dense cross-links cause strong interactions and lead to fast component relaxation and hence small T_2 values, this is well supported by the data presented in Table 3 ($T_{2r} > T_{2i} > T_{2m}$). All samples have identical T_{2r} values, which suggests structures of the rigid phase are not very different for these samples. Very small numerical values of T_{2r} further indicate they correspond to γ-CD clusters mediated by extensive hydrogen bonding. Since γ-CDs are threaded on PDMS, these clusters must also contain small fractions of PDMS strands (Figure 4). T_{2i} values, on the other hand, are a manifestation of the relaxation of intermediate components. In comparison with rigid components, these intermediate components have larger T_2 values, suggesting they possibly correspond to PDMS richer γ-CD clusters. In these clusters, hydrogen bonds are partially disrupted by the presence of PDMS strands, and dipolar couplings are reduced within these clusters. T_{2m} values listed in Table 3 are close to the T_{2m} value of the CR sample, suggesting these T_{2m} values originate from relaxations of bare PDMS strands between cross-links. T_{2i} values of ER1-ER4 are close, and they are considerably smaller than that of the ER5. Since large T_{2i} suggests an intermediate phase which is less densely packed, T_{2i} values in Table 3 therefore indicate the intermediate phase of ER5 is softer and more mobile. This indication has indeed been confirmed by the component fraction values presented in Table 3, from which we can see that ER5 has the lowest mobile phase fraction (33%). The mobile phase fraction of ER5 is only half of that for ER4. Since the mobile phase for ERs is PDMS, a low mobile phase fraction suggests more PDMS in the intermediate phase. Since PDMS strands are flexible and stop γ-CDs from packing closely, the presence of PDMS at a very high level leads to a less rigid intermediate phase for ER5. ^{1}H−^{1}H dipolar couplings are reduced in this more mobile intermediate phase and lead to a much larger T_{2i} value for ER5.

MQ-NMR tests were further performed to investigate ER1-ER5, and the results are shown in Figure 10. The MQ-NMR test of CR without γ-CD was also performed, and the results are shown in Figure S10. MQ-NMR probes chain dynamics at a relatively longer time scale (~100 μs), so the dynamics of PDMS strands in ERs could be studied. In Figure 10a, $I_{n\mathrm{DQ}}$ signals initially rise with DQ evolution time for each sample and later reach a plateau with a normalized intensity of 0.5. The rate of the initial signal rise is known to be related to the density of confinements (cross-links and entanglements), and fitting this initial rising gives residual dipolar coupling D_{res} (Figure 10b). Residual dipolar couplings (D_{res}) are proportionally related to the density of confinements (entanglements and cross-links).[53−55] Network with larger D_{res} has stronger chain interactions and usually is densely cross-linked or entangled. By comparing the curves in Figure 10a, we can see that the rise rate is not too different for each sample. The fact that the D_{res} value of CR is not too different from the D_{res} value of ERs indicates threaded γ-CDs mainly located at the end of the PDMS chain. If γ-CDs are randomly distributed along the PDMS chain and form cross-links with each other by

https://doi.org/10.1021/acspolymersau.4c00096
ACS Polym. Au 2025, 5, 162−173

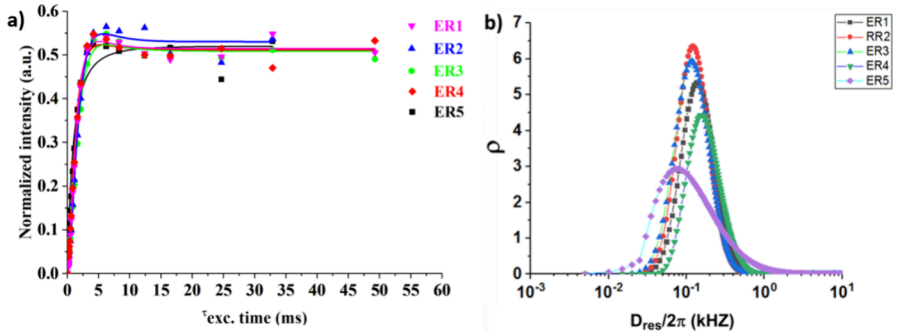

Figure 10. (a) Normalized DQ (n_{DQ}) signals obtained through a point-by-point normalization procedure for ER1-ER5. (b) Residual dipolar coupling distributions of ERs obtained by analysis of the normalized build-up curve I_{nDQ} with fitting.

hydrogen bonding, these cross-links would split the original chain into smaller segments and strongly suppress chain fluctuations. This would give D_{res} that systematically increases with γ-CD content, which is in disagreement with the results shown in Figure 10b. Actually, during PR preparation, even though the hydrogen bonds were temporally disrupted by dissolution in water, they must quickly rebuild when γ-CDs are separated out from the water and threaded into PDMS chains; these hydrogen-bonded clusters therefore mainly reside at the ends of the PDMS chain, so a strong dependence of D_{res} on γ-CD content is not observed. Due to the strong hydrogen bonding interactions between γ-CDs, we can tacitly assume they are closely packed at the end of PDMS chains so the bare chain length does not vary much from sample to sample. This assumption is reasonable as the closely packed γ-CD only covers 18% of the PDMS strand even for the sample (ER5) with the highest γ-CD loading. Since the number of entanglements per chain depends on bare chain length, we therefore can assume the entanglement effects on MQ-NMR observables are the same. Actually, these PDMS chains are lightly entangled with only about two entanglements per chain (M_e = 12 kDa), the amplitude of the constraining effect is therefore dominated by the functionality of the cross-links. However, while the ideal cross-links created by TDMS have a functionality of four, cross-links formed by γ-CDs are irregular and their functionalities are difficult to determine. Therefore, instead of quantifying the constraining effects on PDMS strands from γ-CD clusters, here we would only say that small variations of D_{res} values shown in Figure 10b are reflections of how the movement of PDMS strands is suppressed by end γ-CD clusters.

Another useful parameter that could also be extracted from the I_{nDQ} build-up curve (Figure 10b) by fitting is the standard deviation (σ) of D_{res} (Table 4). For polymer networks, the σ value arises because the networks usually are spatially inhomogeneous and have a distribution of coupling constants.[54] Larger σ suggests a network with a wider distribution of D_{res} and usually is found for a less homogeneous network. Of the five samples, ER5 is the most inhomogeneous with the largest σ, while the other four samples have very close σ values. For ER1-ER4 and CR, by combining the D_{res} results in Figure 10b and σ values in Table 4, we can conclude that the mobile PDMS networks are similar in structure for these samples, mainly composed of PDMS chains cross-linked at two ends. For ER5, a considerably larger σ value can be explained as follows: ER5 has a very high content of intermediate phase which has a relaxation time of about 140 μs, aside from the mobile network composed of end-cross-linked PDMS, this intermediate phase is also contributing to the D_{res} value since DQ-NMR probes chain dynamics at a time scale of ∼100 μs.[56] This intermediate phase, as its T_{2i} value in Table 3 indicates, is different in structure from the mobile phase. Significant broadening of the D_{res} distribution is therefore observed for ER5. Note DQ NMR experiments give access to much slower relaxation processes (0.1−3 ms), that is to say, the structure of DQ NMR experiment probes is the network mainly composed of PDMS chains.[47] The rigid rotaxane aggregates are largely invisible in the DQ NMR experiment because of their much faster decay within 0.02 ms (Table 3).

Table 4. Standard Deviations of D_{res} (σ) for ERs and CR

sample	σ
E1	0.48
E2	0.47
E3	0.51
E4	0.56
E5	1.20
CR	0.54

CONCLUSIONS

A simple two-step method was developed in this work to prepare rotaxanated silicone elastomers. In contrast to traditional rotaxanated elastomers whose stretchability is achieved at the cost of mechanical strength, this new design gives elastomers with both moderate mechanical strength and excellent stretchability. Investigations of these elastomers with NMR techniques show that these elastomers are highly heterogeneous with several types of cross-links contributing to their elasticity. Further investigation of these elastomers with cyclic stress−strain tests shows that the large extension ratio is a result of hydrogen bond reorganization under stress (Mullins effect).

ASSOCIATED CONTENT

Supporting Information

The Supporting Information is available free of charge at https://pubs.acs.org/doi/10.1021/acspolymersau.4c00096.

Synthesis of PRs, BRs and ERs, characterization data for BRs, and PRs and ERs (PDF)

https://doi.org/10.1021/acspolymersau.4c00096
ACS Polym. Au 2025, 5, 162−173

AUTHOR INFORMATION

Corresponding Author

Tao Xing − *Shock and Vibration of Engineering Materials and Structures Key Laboratory of Sichuan Province, Mianyang 621999, China*; orcid.org/0000-0002-9477-2030; Email: 412xingt@caep.cn

Authors

Jiajun Ma − *Shock and Vibration of Engineering Materials and Structures Key Laboratory of Sichuan Province, Mianyang 621999, China*

Wen-cong Xu − *Shock and Vibration of Engineering Materials and Structures Key Laboratory of Sichuan Province, Mianyang 621999, China*

Yangguang Xu − *Applied Mechanics and Structure Safety Key Laboratory of Sichuan Province, School of Mechanics and Aerospace Engineering, Southwest Jiaotong University, Chengdu 611756, China*

Complete contact information is available at: https://pubs.acs.org/10.1021/acspolymersau.4c00096

Author Contributions

The manuscript was written through contributions of all authors. All authors have given approval to the final version of the manuscript. CRediT: **Tao Xing** conceptualization, data curation, resources, supervision; **Jiajun Ma** data curation; **Wen-cong Xu** data curation, formal analysis; **Yangguang Xu** formal analysis, validation.

Funding

The author would like to thank the Natural Science Foundation of China for financial support (Nos. 22475200 and 12172343).

Notes

The authors declare no competing financial interest.

ACKNOWLEDGMENTS

We would like to thank Prof. Kay Saalwächter for pointing us to the log-normal distribution.

REFERENCES

(1) Harada, A.; Takashima, Y.; Yamaguchi, H. Cyclodextrin-based supramolecular polymers. *Chem. Soc. Rev.* **2009**, *38* (4), 875−882.

(2) Noda, Y.; Hayashi, Y.; Ito, K. From topological gels to slide-ring materials. *J. Appl. Polym. Sci.* **2014**, *131* (15), 40509.

(3) Ito, K. Slide-ring materials using topological supramolecular architecture. *Curr. Opin. Solid ST M* **2010**, *14* (2), 28−34.

(4) Mayumi, K.; Ito, K.; Kato, K. *Polyrotaxane and slide-ring materials*; Royal Society of Chemistry: 2015.

(5) Harada, A.; Li, J.; Kamachi, M. Preparation and properties of inclusion complexes of polyethylene glycol with. alpha.-cyclodextrin. *Macromolecules* **1993**, *26* (21), 5698−5703.

(6) Araki, J.; Zhao, C.; Ito, K. Efficient production of polyrotaxanes from α-cyclodextrin and poly (ethylene glycol). *Macromolecules* **2005**, *38* (17), 7524−7527.

(7) Michishita, T.; Okada, M.; Harada, A. Complex formation of polybutadiene with cyclodextrins. *Macromol. Rapid Commun.* **2001**, *22* (10), 763−767.

(8) Akae, Y.; Iijima, K.; Tanaka, M.; Tarao, T.; Takata, T. Main Chain-Type Polyrotaxanes Derived from Cyclodextrin-Based Pseudo [3] rotaxane Diamine and Macromolecular Diisocyanate: Synthesis, Modification, and Characterization. *Macromolecules* **2020**, *53* (6), 2169−2176.

(9) Xie, Z. H.; Rong, M. Z.; Zhang, M. Q.; Liu, D. Implementation of the pulley effect of polyrotaxane in transparent bulk polymer for simultaneous strengthening and toughening. *Macromol. Rapid Commun.* **2020**, *41* (22), No. 2000371.

(10) Gotoh, H.; Liu, C.; Imran, A. B.; Hara, M.; Seki, T.; Mayumi, K.; Ito, K.; Takeoka, Y. Optically transparent, high-toughness elastomer using a polyrotaxane cross-linker as a molecular pulley. *Sci. Adv.* **2018**, *4* (10), No. eaat7629.

(11) Ito, K. Novel entropic elasticity of polymeric materials: why is slide-ring gel so soft? *Polym. J.* **2012**, *44* (1), 38−41.

(12) Yasuda, Y.; Masumoto, T.; Mayumi, K.; Toda, M.; Yokoyama, H.; Morita, H.; Ito, K. Molecular dynamics simulation and theoretical model of elasticity in slide-ring gels. *ACS Macro.Lett.* **2020**, *9* (9), 1280−1285.

(13) Kato, K.; Ikeda, Y.; Ito, K. Direct determination of cross-link density and its correlation with the elastic modulus of a gel with slidable cross-links. *ACS Macro.Lett.* **2019**, *8* (6), 700−704.

(14) Jiang, L.; Liu, C.; Mayumi, K.; Kato, K.; Yokoyama, H.; Ito, K. Highly Stretchable and Instantly Recoverable Slide-Ring Gels Consisting of Enzymatically Synthesized Polyrotaxane with Low Host Coverage. *Chem. Mater.* **2018**, *30* (15), 5013−5019.

(15) Koyanagi, K.; Takashima, Y.; Yamaguchi, H.; Harada, A. Movable Cross-Linked Polymeric Materials from Bulk Polymerization of Reactive Polyrotaxane Cross-Linker with Acrylate Monomers. *Macromolecules* **2017**, *50* (15), 5695−5700.

(16) Jiang, L.; Kato, K.; Mayumi, K.; Yokoyama, H.; Ito, K. One-pot synthesis and characterization of polyrotaxane−silica hybrid aerogel. *ACS Macro.Lett.* **2017**, *6* (3), 281−286.

(17) Mark, J. E.; Schaefer, D. W.; Lin, G. *The polysiloxanes*; Oxford University Press: 2015.

(18) Kato, K.; Inoue, K.; Kidowaki, M.; Ito, K. Organic−inorganic hybrid slide-ring gels: polyrotaxanes consisting of poly (dimethylsiloxane) and γ-cyclodextrin and subsequent topological cross-linking. *Macromolecules* **2009**, *42* (18), 7129−7136.

(19) Tran, J.-A.; Madsen, J.; Skov, A. L. Novel polyrotaxane cross-linkers as a versatile platform for slide-ring silicone. *Bioinspir. Biomim.* **2021**, *16* (2), No. 025002.

(20) Bin Imran, A.; Esaki, K.; Gotoh, H.; Seki, T.; Ito, K.; Sakai, Y.; Takeoka, Y. Extremely stretchable thermosensitive hydrogels by introducing slide-ring polyrotaxane cross-linkers and ionic groups into the polymer network. *Nat. Commun.* **2014**, *5* (1), 5124.

(21) Inomata, A.; Sakai, Y.; Zhao, C.; Ruslim, C.; Shinohara, Y.; Yokoyama, H.; Amemiya, Y.; Ito, K. Crystallinity and cooperative motions of cyclic molecules in partially threaded solid-state polyrotaxanes. *Macromolecules* **2010**, *43* (10), 4660−4666.

(22) Okumura, H.; Okada, M.; Kawaguchi, Y.; Harada, A. Complex Formation between Poly (dimethylsiloxane) and Cyclodextrins: New Pseudo-Polyrotaxanes Containing Inorganic Polymers. *Macromolecules* **2000**, *33* (12), 4297−4298.

(23) Rubinstein, M.; Colby, R. H. *Polymer Physics*; Oxford University Press: 2003.

(24) Maus, A.; Hertlein, C.; Saalwächter, K. A robust proton NMR method to investigate hard/soft ratios, crystallinity, and component mobility in polymers. *Macromol. Chem. Phys.* **2006**, *207* (13), 1150−1158.

(25) Bärenwald, R.; Champouret, Y.; Saalwächter, K.; Schäler, K. Determination of chain flip rates in poly (ethylene) crystallites by solid-state low-field 1H NMR for two different sample morphologies. *J. Phys. Chem. B* **2012**, *116* (43), 13089−13097.

(26) Zhang, R.; Yu, S.; Chen, S.; Wu, Q.; Chen, T.; Sun, P.; Li, B.; Ding, D. Reversible cross-linking, microdomain structure, and heterogeneous dynamics in thermally reversible cross-linked polyurethane as revealed by solid-state NMR. *J. Phys. Chem. B* **2014**, *118* (4), 1126−1137.

(27) Saalwächter, K.; Sommer, J.-U. NMR Reveals Non-Distributed and Uniform Character of Network Chain Dynamics. *Macromol. Rapid Commun.* **2007**, *28* (14), 1455−1465.

(28) Saalwächter, K. Detection of Heterogeneities in Dry and Swollen Polymer Networks by Proton Low-Field NMR Spectroscopy. *J. Am. Chem. Soc.* **2003**, *125* (48), 14684−14685.
(29) Saalwächter, K.; Herrero, B.; López-Manchado, M. A. Chain Order and Cross-Link Density of Elastomers As Investigated by Proton Multiple-Quantum NMR. *Macromolecules* **2005**, *38* (23), 9650−9660.
(30) Zou, X.; Kui, X.; Zhang, R.; Zhang, Y.; Wang, X.; Wu, Q.; Chen, T.; Sun, P. Viscoelasticity and Structures in Chemically and Physically Dual-Cross-Linked Hydrogels: Insights from Rheology and Proton Multiple-Quantum NMR Spectroscopy. *Macromolecules* **2017**, *50* (23), 9340−9352.
(31) Okumura, H.; Kawaguchi, Y.; Harada, A. Preparation and characterization of inclusion complexes of poly (dimethylsiloxane) s with cyclodextrins. *Macromolecules* **2001**, *34* (18), 6338−6343.
(32) Kihara, N.; Hinoue, K.; Takata, T. Solid-State End-Capping of Pseudopolyrotaxane Possessing Hydroxy-Terminated Axle to Polyrotaxane and Its Application to the Synthesis of a Functionalized Polyrotaxane Capable of Yielding a. *Macromolecules* **2005**, *38* (2), 223−226.
(33) Kato, K.; Komatsu, H.; Ito, K. A versatile synthesis of diverse polyrotaxanes with a dual role of cyclodextrin as both the cyclic and capping components. *Macromolecules* **2010**, *43* (21), 8799−8804.
(34) Laws, D. D.; Bitter, H. M. L.; Jerschow, A. Solid-state NMR spectroscopic methods in chemistry. *Angew. Chem., Int. Ed.* **2002**, *41* (17), 3096−3129.
(35) Sawada, J.; Aoki, D.; Uchida, S.; Otsuka, H.; Takata, T. Synthesis of vinylic macromolecular rotaxane cross-linkers endowing network polymers with toughness. *ACS Macro Lett.* **2015**, *4* (5), 598−601.
(36) Kato, K.; Nemoto, K.; Mayumi, K.; Yokoyama, H.; Ito, K. Ductile Glass of Polyrotaxane Toughened by Stretch-Induced Intramolecular Phase Separation. *ACS Appl. Mater.* **2017**, *9* (38), 32436−32440.
(37) Hanson, D. E.; Hawley, M.; Houlton, R.; Chitanvis, K.; Rae, P.; Orler, E. B.; Wrobleski, D. A. Stress softening experiments in silica-filled polydimethylsiloxane provide insight into a mechanism for the Mullins effect. *Polymer* **2005**, *46* (24), 10989−10995.
(38) Liang, X.; Nakajima, K. Study of the Mullins Effect in Carbon Black-Filled Styrene−Butadiene Rubber by Atomic Force Microscopy Nanomechanics. *Macromolecules* **2022**, *55* (14), 6023−6030.
(39) Merabia, S.; Sotta, P.; Long, D. R. A Microscopic Model for the Reinforcement and the Nonlinear Behavior of Filled Elastomers and Thermoplastic Elastomers (Payne and Mullins Effects). *Macromolecules* **2008**, *41* (21), 8252−8266.
(40) Hagita, K.; Murashima, T. Critical Importance of Both Bond Breakage and Network Heterogeneity in Hysteresis Loop on Stress−Strain Curves and Scattering Patterns. *Macromolecules* **2024**, *57* (23), 10903−10911.
(41) Patel, S. K.; Malone, S.; Cohen, C.; Gillmor, J. R.; Colby, R. H. Elastic modulus and equilibrium swelling of poly (dimethylsiloxane) networks. *Macromolecules* **1992**, *25* (20), 5241−5251.
(42) Nishimura, Y.; Chung, J.; Muradyan, H.; Guan, Z. Silyl Ether as a Robust and Thermally Stable Dynamic Covalent Motif for Malleable Polymer Design. *J. Am. Chem. Soc.* **2017**, *139* (42), 14881−14884.
(43) Sample, C. S.; Lee, S.-H.; Li, S.; Bates, M. W.; Lensch, V.; Versaw, B. A.; Bates, C. M.; Hawker, C. J. Metal-Free Room-Temperature Vulcanization of Silicones via Borane Hydrosilylation. *Macromolecules* **2019**, *52* (19), 7244−7250.
(44) Yan, X.; Bai, L.; Feng, B.; Zheng, J. Mechanically strong, thermally stable, and reprocessable poly (dimethylsiloxane) elastomers enabled by dynamic silyl ether linkages. *Eur. Polym. J.* **2022**, *173* (23), No. 111267.
(45) Gao, Y.; Zhang, R.; Lv, W.; Liu, Q.; Wang, X.; Sun, P.; Winter, H. H.; Xue, G. Critical Effect of Segmental Dynamics in Polybutadiene/Clay Nanocomposites Characterized by Solid State 1H NMR Spectroscopy. *J. Phys. Chem. C* **2014**, *118* (10), 5606−5614.
(46) Malmierca, M. A.; González-Jiménez, A.; Mora-Barrantes, I.; Posadas, P.; Rodríguez, A.; Ibarra, L.; Nogales, A.; Saalwächter, K.; Valentín, J. L. Characterization of Network Structure and Chain Dynamics of Elastomeric Ionomers by Means of 1H Low-Field NMR. *Macromolecules* **2014**, *47* (16), 5655−5667.
(47) Papon, A.; Saalwächter, K.; Schäler, K.; Guy, L.; Lequeux, F.; Montes, H. Low-field NMR investigations of nanocomposites: polymer dynamics and network effects. *Macromolecules* **2011**, *44* (4), 913−922.
(48) Zhang, R.; Yan, T.; Lechner, B.-D.; Schröter, K.; Liang, Y.; Li, B.; Furtado, F.; Sun, P.; Saalwächter, K. Heterogeneity, Segmental and Hydrogen Bond Dynamics, and Aging of Supramolecular Self-Healing Rubber. *Macromolecules* **2013**, *46* (5), 1841−1850.
(49) Orza, R. A.; Magusin, P. C.; Litvinov, V. M.; van Duin, M.; Michels, M. Solid-state 1H NMR study on chemical cross-links, chain entanglements, and network heterogeneity in peroxide-cured EPDM rubbers. *Macromolecules* **2007**, *40* (25), 8999−9008.
(50) Litvinov, V. EPDM/PP thermoplastic vulcanizates as studied by proton NMR relaxation: phase composition, molecular mobility, network structure in the rubbery phase, and network heterogeneity. *Macromolecules* **2006**, *39* (25), 8727−8741.
(51) Messinger, R.; Marks, T.; Gleiman, S.; Milstein, F.; Chmelka, B. Molecular origins of macroscopic mechanical properties of elastomeric organosiloxane foams. *Macromolecules* **2015**, *48* (14), 4835−4849.
(52) Litvinov, V. M.; Dias, A. A. Analysis of Network Structure of UV-Cured Acrylates by 1H NMR Relaxation, 13C NMR Spectroscopy, and Dynamic Mechanical Experiments. *Macromolecules* **2001**, *34* (12), 4051−4060.
(53) Chassé, W.; Lang, M.; Sommer, J.-U.; Saalwächter, K. Cross-Link Density Estimation of PDMS Networks with Precise Consideration of Networks Defects. *Macromolecules* **2012**, *45* (2), 899−912.
(54) Chassé, W.; Schlögl, S.; Riess, G.; Saalwächter, K. Inhomogeneities and local chain stretching in partially swollen networks. *Soft Matter* **2013**, *9* (29), 6943−6954.
(55) Zhang, R.; Zhang, C.; Yang, Z.; Wu, Q.; Sun, P.; Wang, X. Hierarchical Dynamics in a Transient Polymer Network Cross-Linked by Orthogonal Dynamic Bonds. *Macromolecules* **2020**, *53* (14), 5937−5949.
(56) Syed, I. H.; Stratmann, P.; Hempel, G.; Klüppel, M.; Saalwächter, K. Entanglements, Defects, and Inhomogeneities in Nitrile Butadiene Rubbers: Macroscopic versus Microscopic Properties. *Macromolecules* **2016**, *49* (23), 9004−9016.

https://doi.org/10.1021/acspolymersau.4c00096
ACS Polym. Au 2025, 5, 162−173